

Electronic Supporting Information

Muscle-Inspired Capacitive Tactile Sensors with Superior Sensitivity in an Ultra-wide Stress Range

Muscle-inspired capacitive tactile sensors with superior sensitivity in an ultra-wide stress range

Xiaoping Shen^a, Kangchen Nie^a, Li Zheng^a, Zhe Wang^a, Zhaosong Wang^a, Song Li^a,
Chunde Jin^{a*}, Qingfeng Sun^{a*}

^a School of Engineering, Zhejiang A&F University, Hangzhou 311300, People's Republic of China

*Corresponding authors: Chunde Jin, E-mail: jincd@zafu.edu.cn; Qingfeng Sun, E-mail: qfsun@zafu.edu.cn

EXPERIMENTAL

Preparation of rGO films. 10 g graphite powder was added to a three-necked flask containing 250 mL 98% H₂SO₄ in an ice water bath with vigorous stirring. Then 50 g KMnO₄ was slowly added into the flask while stirring within 2 h. The reaction was proceeded at 35°C for 1 h, followed by stirring at room temperature for 24 h. After reaction, 1 L of preheated (90°C) DI water was slowly added into the mixture. This dilution and exfoliation process was kept at 90°C while stirring for 40 min. The mixture was cooled to room temperature and 3% H₂O₂ was added until no more bubbles were generated. The mixture was then filtered and washed with DI water until the pH value was neutral. Part of the concentrated mixture was taken and the concentration was diluted to 5 mg mL⁻¹. The diluted suspension was then ultrasonicated for 20 min at an output power of 1000W. Part of the resulting homogeneous suspension (20 mL) was transferred to a crystallizing dish with a 90 mm inner diameter. The dish was put in an oven for evaporation at 70°C to obtain a GO film. This film was finally soaked in 20 mL 57% HI at room temperature for 6 h for reduction, followed by washing and drying to obtain the rGO film.

Muscle-Inspired Capacitive Tactile Sensors with Superior Sensitivity in an Ultra-wide Stress Range

Characterization. ^1H NMR spectrum of VImPS was acquired at 298 K with a Bruker Avance III 600 MHz NMR spectrometer (Bruker Biospin, Rheinstetten, Germany) at a frequency of 600 MHz. X-ray diffraction patterns (XRD) of all samples were recorded on a Bruker D8 Advance, Japan at 40 kV (100 mA) with Cu $K\alpha$ radiation ($\lambda=1.5406$ Å). Functional groups analyses of all samples were processed with attenuated total reflection-Fourier transform infrared spectroscopy (ATR-FTIR; Nicolet IS10, USA). The structure of rGO was detected by transmission electron microscopy (TEM, FEI Tecnai G2 F20, USA) and Raman spectra (Renishaw inVia, UK).

RESULTS AND DISCUSSION

BJH method

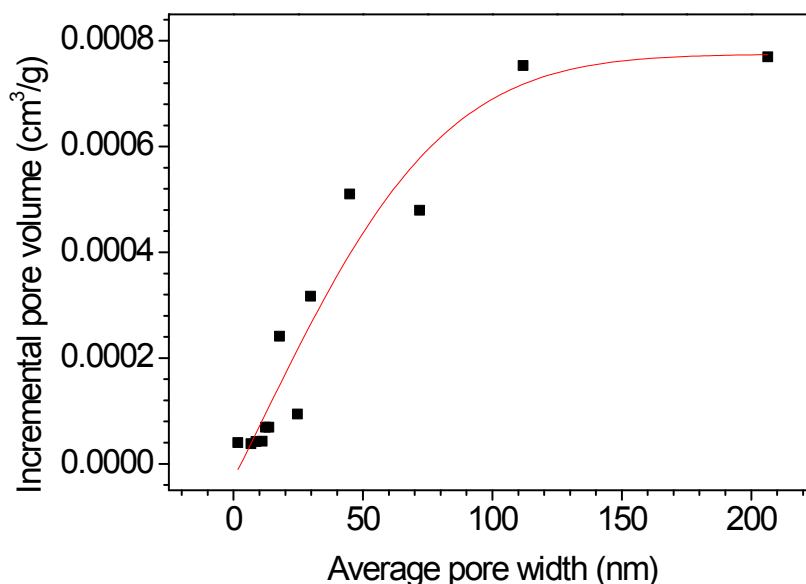


Figure S1. The pore size distribution of WA using the BJH method.

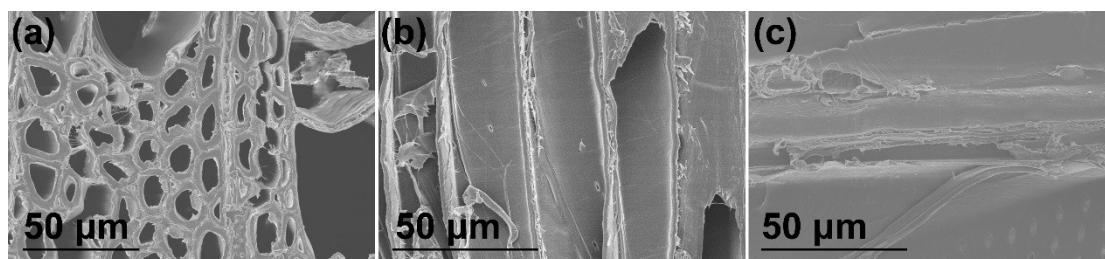
SEM images

Figure S2. The SEM images of the (a) cross-section, (b) radial section and (c) tangential section of poplar wood.

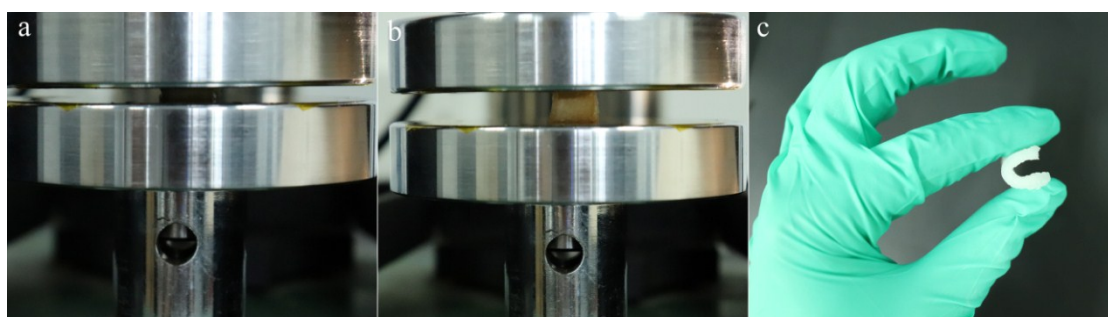
Appearances of WA/PIL hydrogels

Figure S3. The appearances of bulk tan 1.0 after (a) loading and (b) unloading, and (c) the distorted hydrogel sheet.

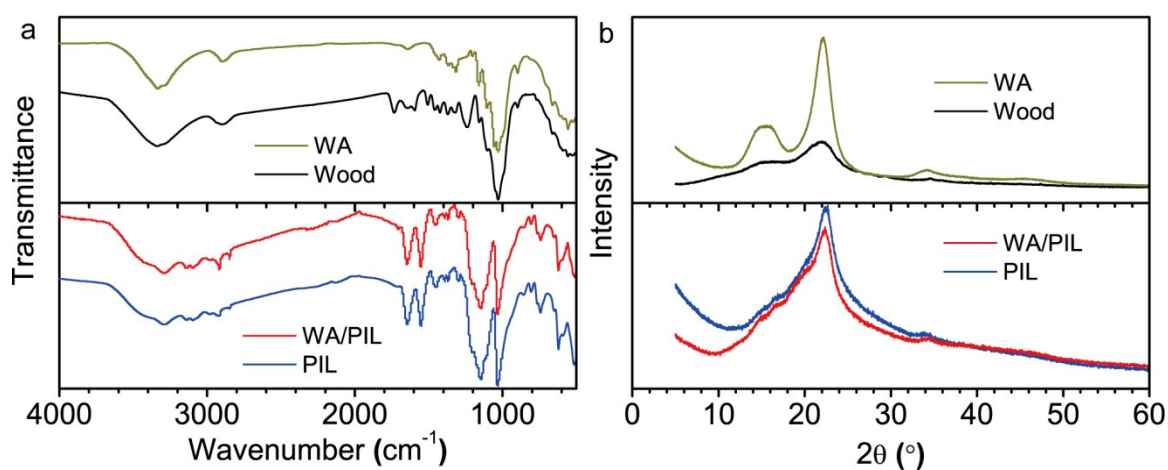
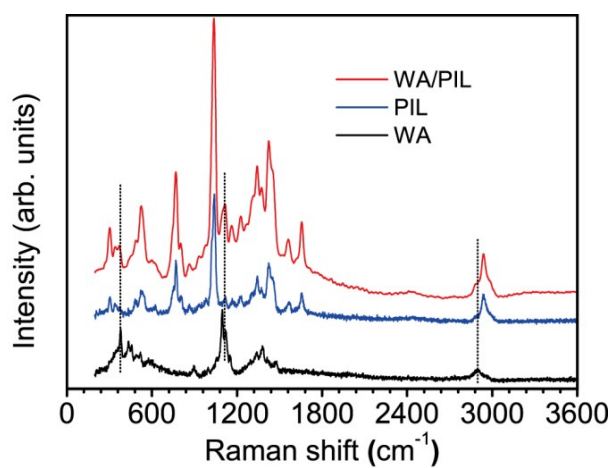
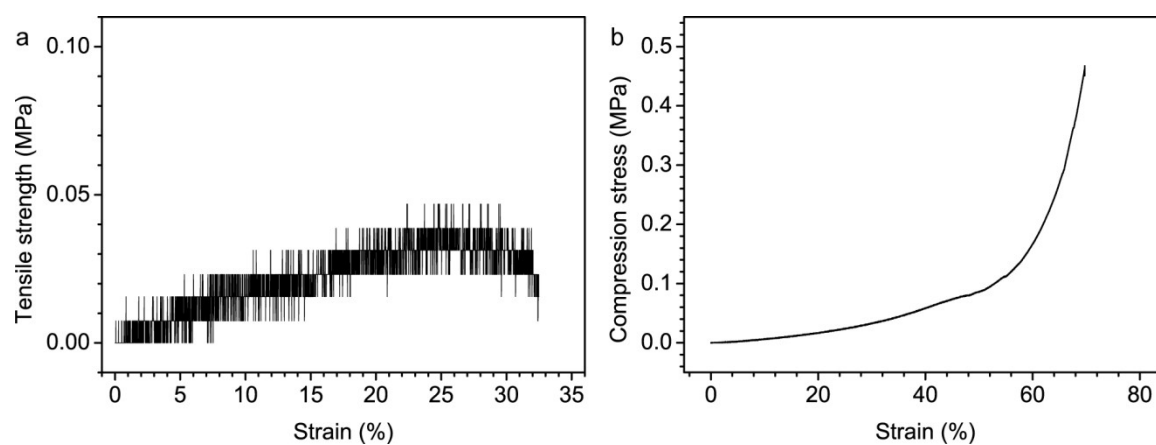
FT-IR and XRD

Figure S4. (a) FT-IR spectra and (b) XRD diffractograms of wood, WA, PIL and WA/PIL.

Raman spectra**Figure S5.** Raman spectra of the WA/PIL hydrogel.**Mechanical properties of PIL****Figure S6.** Tensile and compressive strength of the pure PIL hydrogel (with a 1.0 mol% BIS content).

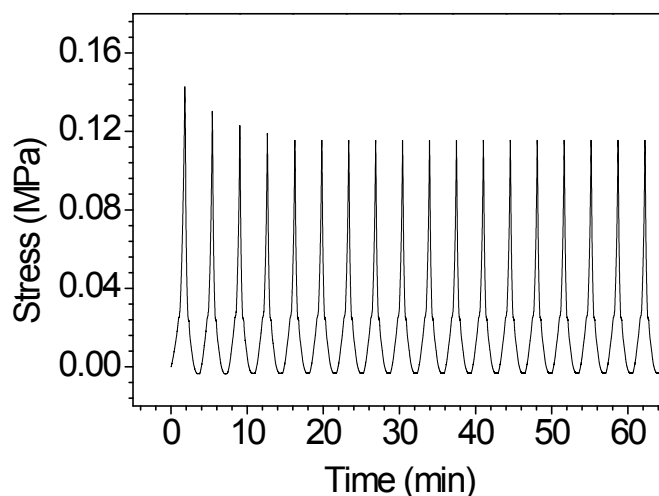
Loading-unloading cycles

Figure S7. The loading-unloading compression cycles of the tangential WA/PIL hydrogel ($\tan 1.0$) at a 40% compression strain.

rGO analyses

The rGO film prepared with the Hummers' method^{1,2} was thin (*ca.* 0.01 μm) and crumpled, and the selected area electron diffraction (SAED) pattern showed clear diffraction spots with a six-fold hexagonal lattice pattern, indicating the successful and partial reduction of rGO³. The resulting rGO exhibited a broad diffraction peak at 23.9° corresponding to the (002) plane of rGO and a G band (the E_{2g} mode of sp² carbon atoms) at 1591.5 cm^{-1} and a D band (the symmetry A_{1g} mode) at 1349.5 cm^{-1} in the Raman spectrum, which were also conformed to the characteristics of rGO³⁻⁵.

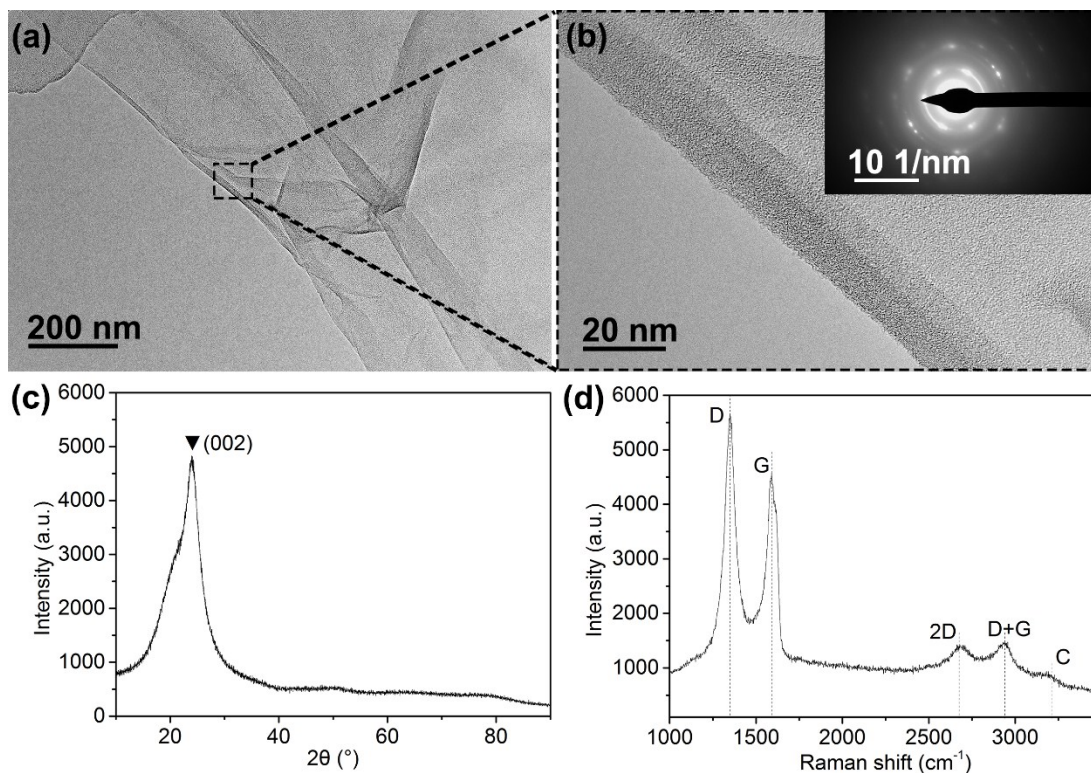


Figure S8. (a) TEM, (b) HRTEM (insert image: SAED), (c) XRD and (d) Raman spectrum of the rGO film.

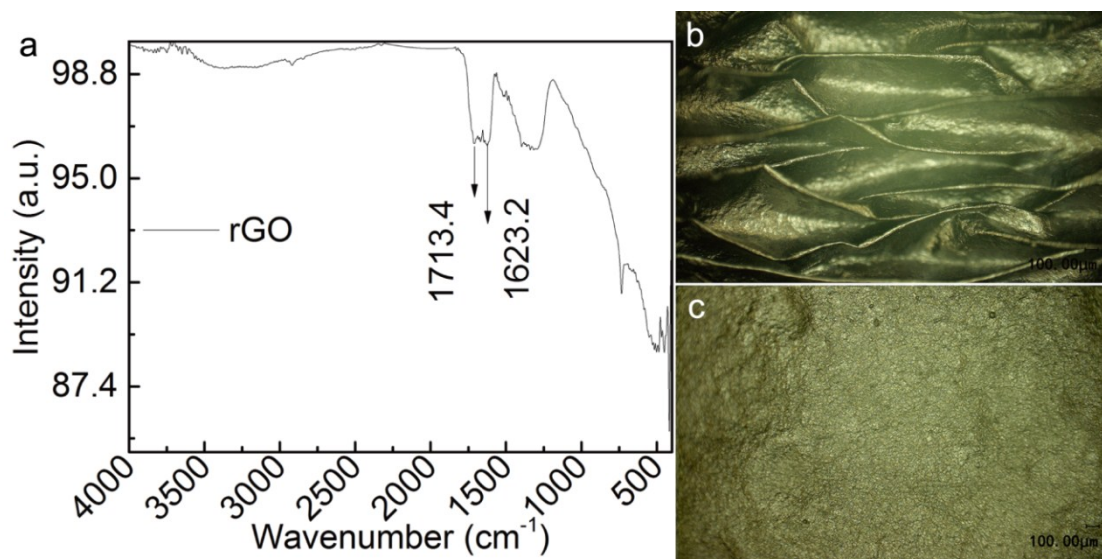
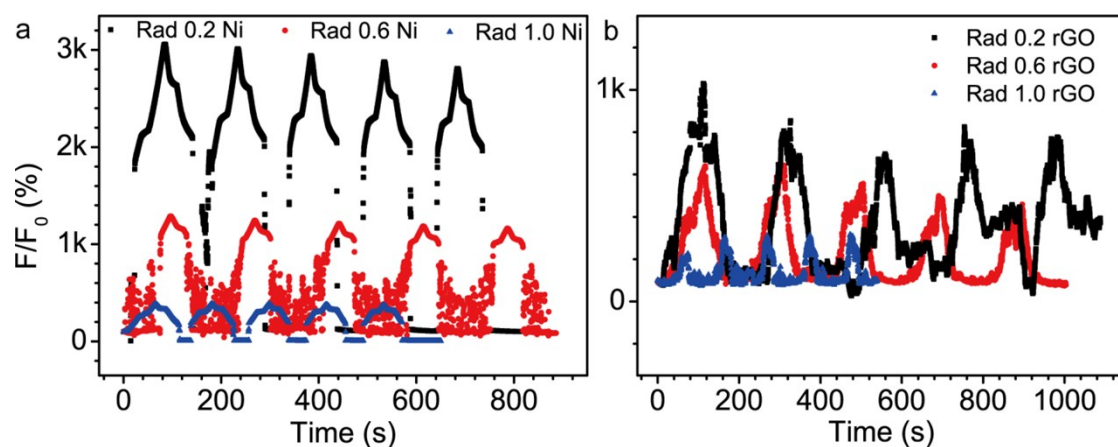


Figure S9. (a) FT-IR spectrum and 3D microscope photos of (b) the wrinkled rGO film and (c) the flat rGO film (Note: the Ni foam was basically the same as the flat rGO). The peaks at 1713 cm^{-1} and 1623.2 cm^{-1} were assigned to the stretching vibrations of C=O and C=C, which indicated the partial reduction of the rGO⁴.

Table S1 Results of the conductivity values of the hydrogels and electrodes measured by Four-Point Probes.

Samples	Thickness (mm)	Resistance (Ω)	Resistivity ($\Omega\cdot\text{mm}$)	Conductivity (S/mm)
tan 0.2	2	2219	4438	2.3×10^{-4}
tan 0.6	2	291	582	1.7×10^{-3}
tan 1.0	2	85	170	5.9×10^{-3}
rGO	0.01	13	0.130	7.692
Ni	0.1	4×10^{-3}	4×10^{-4}	2.5×10^3

Capacitance responsive signals**Figure S10.** Capacitance-time curves as a function of linear deformation of the radial WA/PIL

hydrogels using (a) Ni and (b) rGO electrodes.

Muscle-Inspired Capacitive Tactile Sensors with Superior Sensitivity in an Ultra-wide Stress Range

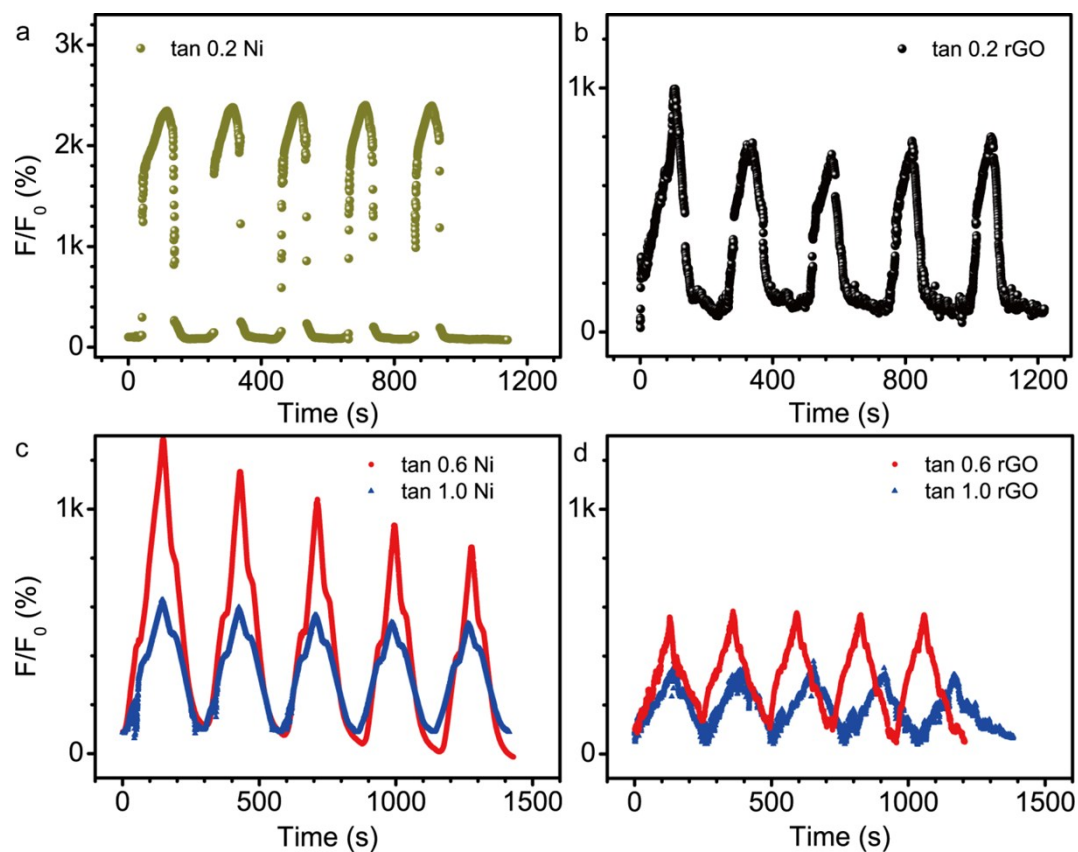


Figure S11. Capacitance-time curves as a function of linear deformation of the tangential WA/PIL hydrogels. (a) $\tan 0.2$ with Ni electrodes, (b) $\tan 0.2$ with rGO electrodes, (c) $\tan 0.6$ and $\tan 1.0$ with Ni electrodes, and (d) $\tan 0.6$ and $\tan 1.0$ with rGO electrodes.

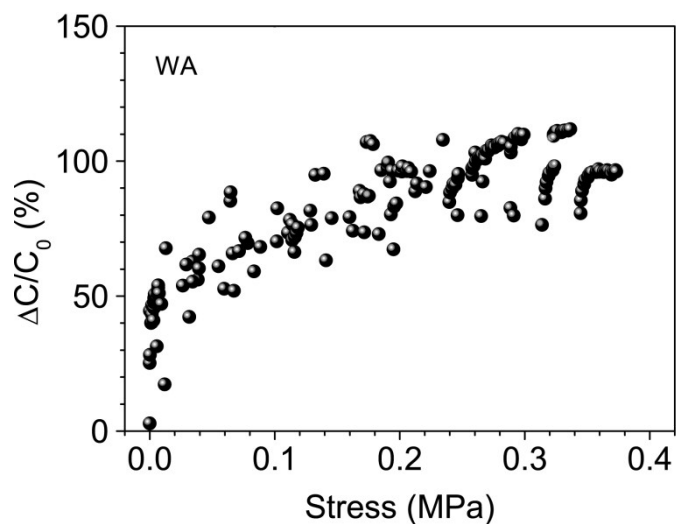
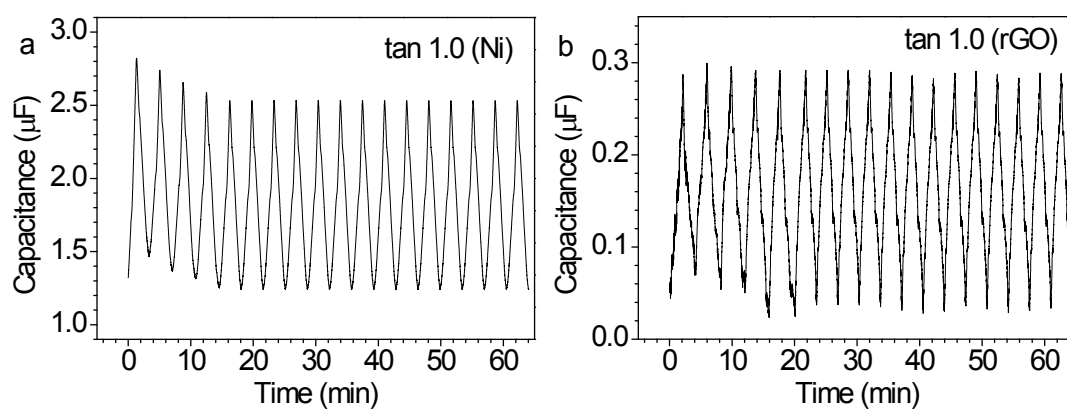
Sensitivity of WA-based sensor

Figure S12. Capacitance change rate-stress curve of WA-based sensor assembled with Ni electrodes.

Table S2 Sensitivity values of WA/PIL hydrogel sensors.

Hydrogel	Electrodes	Max. Stress (MPa)	Sensitivity (MPa ⁻¹)
tan 0.6	Ni	0.07	5.07
		1.00	0.21
	rGO	0.08	14.8
		0.80	0.81
tan 1.0	Ni	0.09	9.67
		1.00	0.33
	rGO	0.13	19.7
		1.10	1.13
WA	Ni	0.07	6.06
		0.38	0.31

Sensing stability**Figure S13.** Sensing stability tests of the tan 1.0 hydrogel sensors with (a) Ni or (b) rGO electrodes upon the compressive stress gradually increasing up to 0.1 MPa.

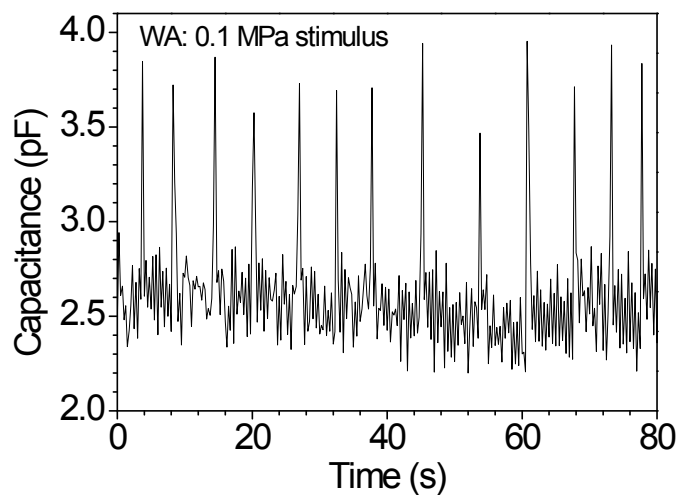


Figure S14. Sensing signals of a WA-based sensor towards 0.1 MPa stimulus using a 1000 g weight ($A_{\text{sensor}} = 100 \text{ mm}^2$).

Durability

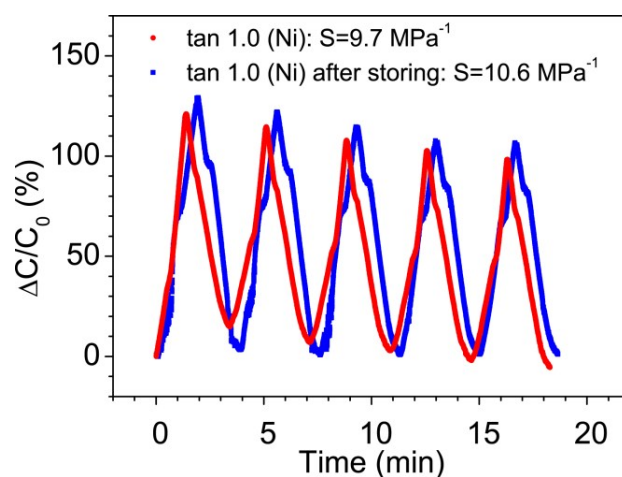


Figure S15. Sensing durability of tan 1.0 (Ni) after storing for one month while sealing.

Responsive time analyses

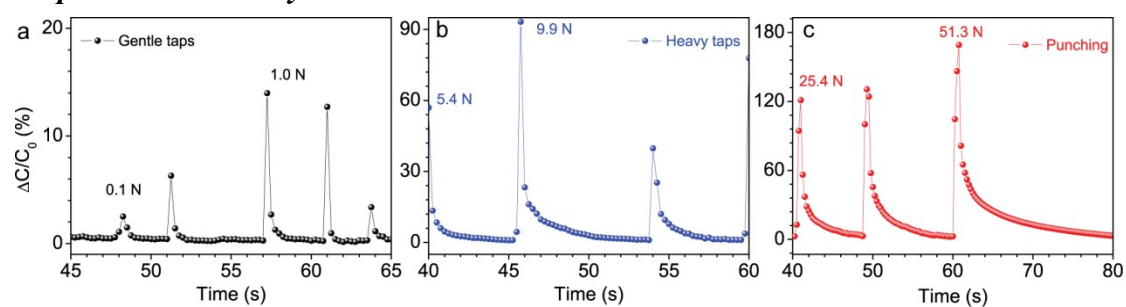


Figure S16. Responsive and recovery time during sensing towards different stimuli.

Wood block

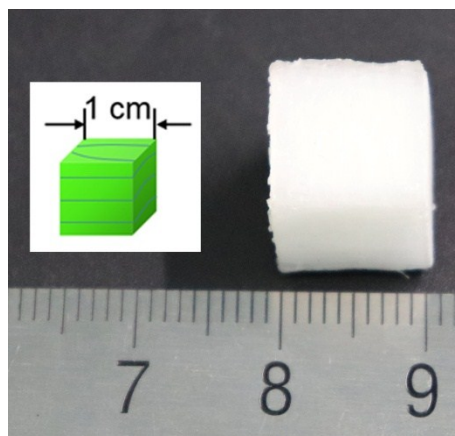


Figure S17. Schematic diagram of the sawn wood block and WA.

$^1\text{H NMR}$

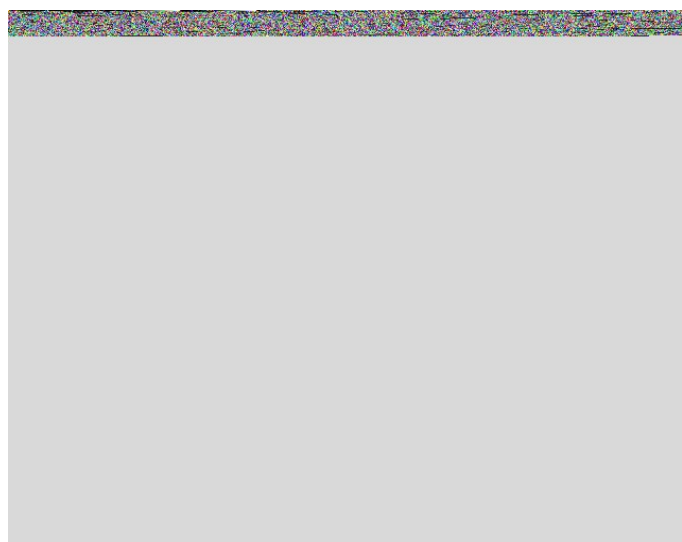


Figure S18. $^1\text{H NMR}$ of the synthesized 3-(1-vinyl-3-imidazolium) propanesulfonate (VImPS).

Electronic Supporting Information

Muscle-Inspired Capacitive Tactile Sensors with Superior Sensitivity in an Ultra-wide Stress Range

Table S3 Comparison of sensitivity and stress ranges of various hydrogel sensors.

Reference	Type of sensor	Materials	Stress range	Sensitivity
6	Capacitive	CNT arrays on PU	20 KPa	0.19 KPa ⁻¹ (<1 KPa) 0.10 KPa ⁻¹ (1–10 KPa) 0.04 KPa ⁻¹ (10–20 KPa)
7	Capacitive	PAAc/alginate/ACC hydrogel	1.0 KPa	0.17 KPa ⁻¹
8	Capacitive	Gelatin DES gel	160 KPa	0.013 KPa ⁻¹
9	Capacitive	PAAm/NaCl hydrogel	40 KPa	0.009 KPa ⁻¹
10	Capacitive	PAAm-LiCl hydrogel	26 KPa	0.006 KPa ⁻¹
11	Capacitive	AgNWs/Ecoflex	1.2 MPa	1.62 MPa ⁻¹ (<0.4 MPa) 0.57 MPa ⁻¹ (<1.2 MPa)
12	Piezoresistive	PVA/PAAc/F-MWCNT/PEDOT	25 KPa	0.011 KPa ⁻¹
13	Piezoresistive	PAniNR@PAN	0.3 MPa	0.95 MPa ⁻¹
14	Piezoresistive	Pt-rGOH aerogel	1.8 MPa	0.3 MPa ⁻¹
15	Piezoresistive	PEI/CNT	40 MPa	0.05 MPa ⁻¹
16	Piezoresistive	cellulose/graphene composites	35 MPa	0.0013 MPa ⁻¹
Our work	Capacitive	Wood/PIL hydrogel	1.2 MPa (70% strain)	9.67 MPa ⁻¹ (<0.092 MPa) 0.33 MPa ⁻¹ (<1.0 MPa)

Abbreviations: carbon nanotube (CNT), polyurethane (PU), polyacrylic acid (PAAc), amorphous calcium carbonate (ACC), deep eutectic solvent (DES), polyacrylamide (PAAm), polyvinyl alcohol (PVA), surfactantfunctionalized multi-walled carbon nanotube (F-MWCNT), poly(3,4-

ethylenedioxythiophene):polystyrene sulfonate (PEDOT:PSS), polyaniline nanorod on polyacrylonitrile (PAN) nanofiber substrate (PAniNR@PAN), Pt/reduced graphene oxide hydrogel (Pt-rGOH), polyethyleneimine (PEI)

References

1. L. Jiang, X. Lu, C. Xie, G. Wan, H. Zhang and T. Youhong, *J. Phys. Chem. C*, 2015, 119, 3903-3910.
2. J. Chen, B. Yao, C. Li and G. Shi, *Carbon*, 2013, 64, 225-229.
3. K. Krishnamoorthy, M. Veerapandian, K. Yun and S. J. Kim, *Carbon*, 2013, 53, 38-49.
4. Y. Guo, X. Sun, Y. Liu, W. Wang, H. Qiu and J. Gao, *Carbon*, 2012, 50, 2513-2523.
5. X. Díez-Betriu, S. Álvarez-García, C. Botas, P. Álvarez, J. Sánchez-Marcos, C. Prieto, R. Menéndez and A. de Andrés, *J. Mater. Chem. C*, 2013, 1, 6905-6912.
6. C. M. Boutry, M. Negre, M. Jorda, O. Vardoulis, A. Chortos, O. Khatib and Z. Bao, *Science Robotics*, 2018, 3, eaau6914.
7. Z. Lei, Q. Wang, S. Sun, W. Zhu and P. Wu, *Adv. Mater.*, 2017, 29.
8. H. Qin, R. E. Oweyung, S. R. Sonkusale and M. J. Panzer, *J. Mater. Chem. C*, 2019, 7, 601-608.
9. J. Y. Sun, C. Keplinger, G. M. Whitesides and Z. Suo, *Adv. Mater.*, 2014, 26, 7608-7614.
10. C. Larson, B. Peele, S. Li, S. Robinson, M. Totaro, L. Beccai, B. Mazzolai and R. Shepherd, *Science*, 2016, 351, 1071-1074.
11. S. Yao and Y. Zhu, *Nanoscale*, 2014, 6, 2345-2352.
12. G. Ge, W. Yuan, W. Zhao, Y. Lu, Y. Zhang, W. Wang, P. Chen, W. Huang, W. Si and X. Dong, *J. Mater. Chem. A*, 2019, 7, 5949-5956.
13. H. H. Shi, N. Khalili, T. Morrison and H. E. Naguib, *ACS Appl. Mater. Interfaces*, 2018, 10, 19037-19046.
14. S.-H. Hwang, Y.-B. Park, S.-H. Hur and H. G. Chae, *ACS Appl. Nano Mater.*, 2018, 1, 2836-2843.
15. S. M. Doshi and E. T. Thostenson, *ACS Sens.*, 2018, 3, 1276-1282.
16. Y. Chen, P. Pötschke, J. Pionteck, B. Voit and H. Qi, *J. Mater. Chem. A*, 2018, 6, 7777-7785.